blood®
Regular Article

MYELOID NEOPLASIA

Posttranscriptional depletion of ribosome biogenesis factors engenders therapeutic vulnerabilities in *NPM1*-mutant AML

Aristi Damaskou,[1,2] Rachael Wilson,[1,2] Malgorzata Gozdecka,[1,2] George Giotopoulos,[1,2] Ryan Asby,[1,2] Maria Eleftheriou,[1-3] Muxin Gu,[1,2] Christian Récher,[4-7] Véronique Mansat-De Mas,[4-7] Francois Vergez,[4-7] Ambrine Sahal,[4-6] Binje Vick,[8,9] Evangelia K. Papachristou,[10] Ashley Sawle,[10] Eliza Yankova,[1-3] Monika Dudek,[1,2] Xiaoxuan Liu,[1,2] James Russell,[1,2] Justyna Rak,[1,2] Christine Hilcenko,[1,2,11,12] Clive D'Santos,[10] Irmela Jeremias,[8,9,13] Jean-Emmanuel Sarry,[4-6] Konstantinos Tzelepis,[1-3] Brian J. P. Huntly,[1,2,11] Alan J. Warren,[1,2,11] Omid Tavana,[14] and George S. Vassiliou[1,2,15]

[1]Cambridge Stem Cell Institute, [2]Department of Haematology, and [3]Milner Therapeutics Institute, University of Cambridge, Cambridge, United Kingdom; [4]Centre de Recherches en Cancérologie de Toulouse, Université de Toulouse, INSERM U1037, Centre National de la Recherche Scientifique U5077, Toulouse, France; [5]LabEx Toucan, Toulouse, France; [6]Équipe Labellisée Ligue Nationale Contre le Cancer 2023, Toulouse, France; [7]Service d'Hématologie, Centre Hospitalier Universitaire de Toulouse, Institut Universitaire du Cancer de Toulouse Oncopole, Toulouse, France; [8]Research Unit Apoptosis in Hematopoietic Stem Cells, Helmholtz Zentrum München, German Research Center for Environmental Health, Munich, Germany; [9]German Cancer Consortium, Partner Site Munich, Munich, Germany; [10]Cancer Research UK Cambridge Institute and [11]Cambridge Institute for Medical Research, University of Cambridge, Cambridge, United Kingdom; [12]Department of Infectious Disease, Imperial College London, London, United Kingdom; [13]Department of Pediatrics, Dr. von Hauner Children's Hospital, University Hospital, Ludwig Maximilian University, Munich, Germany; [14]Hematology R&D, AstraZeneca, Waltham, MA; and [15]Department of Haematology, Cambridge University Hospitals NHS Trust, Cambridge, United Kingdom

KEY POINTS

- **Preleukemic and leukemic *NPM1*-mutant cells have reduced levels of several ribosome biogenesis proteins.**
- **Targeted therapeutic disruption of ribosome biogenesis is a potential strategy against *NPM1*-mutant AML.**

NPM1 is a multifunctional phosphoprotein with key roles in ribosome biogenesis among its many functions. *NPM1* gene mutations drive 30% of acute myeloid leukemia (AML) cases. The mutations disrupt a nucleolar localization signal and create a novel nuclear export signal, leading to cytoplasmic displacement of the protein (NPM1c). *NPM1c* mutations prime hematopoietic progenitors to leukemic transformation, but their precise molecular consequences remain elusive. Here, we first evaluate the effects of isolated *NPM1c* mutations on the global proteome of preleukemic hematopoietic stem and progenitor cells (HSPCs) using conditional knockin *Npm1*$^{cA/+}$ mice. We discover that many proteins involved in ribosome biogenesis are significantly depleted in these murine HSPCs, but also importantly in human *NPM1*-mutant AMLs. In line with this, we found that preleukemic *Npm1*$^{cA/+}$ HSPCs display higher sensitivity to RNA polymerase I inhibitors, including actinomycin D (ActD), compared with *Npm1*$^{+/+}$ cells. Combination treatment with ActD and venetoclax inhibited the growth and colony-forming ability of preleukemic and leukemic NPM1c^{+} cells, whereas low-dose ActD treatment was able to resensitize resistant NPM1c^{+} cells to venetoclax. Furthermore, using data from CRISPR dropout screens, we identified and validated *TSR3*, a 40S ribosomal maturation factor whose knockout preferentially inhibited the proliferation of NPM1c^{+} AML cells by activating a p53-dependent apoptotic response. Similarly, to low-dose ActD treatment, *TSR3* depletion could partially restore sensitivity to venetoclax in therapy-resistant NPM1c^{+} AML models. Our findings propose that targeted disruption of ribosome biogenesis should be explored as a therapeutic strategy against *NPM1*-mutant AML.

Introduction

Nucleophosmin, coded by the *NPM1* gene, is a highly abundant phosphoprotein involved in diverse cellular processes.[1-6] It can shuttle between the nucleus and cytoplasm, but at a steady state, it is primarily located at the nucleolus, the main site of ribosomal RNA (rRNA) transcription and early ribosome biogenesis.[7] More specifically, nucleophosmin is located at the outer, granular component of the nucleolus,[8] contributes to maintaining the organelle's structure,[9,10] and is involved in rRNA 2′-O-methylation.[11]

Somatic mutations affecting the *NPM1* gene are found in ~30% of cases of acute myeloid leukemia (AML)[12,13] and define the most common AML subtype. AML-associated *NPM1* mutations, usually 4-base pair duplications/insertions within the gene's

final exon, disrupt a nucleolar localization signal and create a novel nuclear export signal. As a result, mutant nucleophosmin is aberrantly localized to the cytoplasm (NPM1c) through interaction with XPO1, a major effector of nucleocytoplasmic traffic.[14] The current standard-of-care treatment for patients with *NPM1c*-mutant AML is 3+7 chemotherapy, whereas for patients carrying *FLT3* comutations, such as internal tandem duplications (ITDs), a FLT3 inhibitor is incorporated into the first-line treatment.[15,16] Most patients enter complete remission, but approximately half relapse and most succumb to their disease, highlighting the need for new therapies.[17]

Despite its high prevalence in AML, the molecular consequences of the *NPM1c* mutation are incompletely understood, which poses an obstacle to the design of effective therapeutic strategies.[18] Recent advances have given insights into the transcriptomic and epigenetic effects of *NPM1c* mutations,[19] but less is known about its global posttranscriptional and proteomic consequences.

In this study, we determined the global proteomic consequences of isolated *NPM1c* mutations in preleukemic hematopoietic progenitors from knockin *Npm1c*-mutant mice, which faithfully recapitulate the human mutations.[19-21] We then investigated which changes were also detected in full-blown *NPM1*-mutant AML[22] and evaluated these against CRISPR knockout screens[23-25] to identify potential therapeutic targets. Notably, we found significant decreases in abundance of multiple ribosome biogenesis factors in NPM1c$^+$ preleukemia which were also observed in human NPM1c$^+$ AML and were associated with increased sensitivity to the RNA polymerase (pol) I inhibitor actinomycin D (ActD) alone and particularly in combination with the Bcl-2 inhibitor venetoclax. Focusing on individual targets, we discovered that *NPM1c*-mutant cells are dependent on *TSR3*, a normally nonessential maturation factor of the 40S ribosomal subunit. Finally, we demonstrated that both low-dose ActD treatment and *TSR3* knockout induce resensitization to venetoclax in previously resistant NPM1c$^+$ leukemia cells.

Methods

Also see the supplemental Methods (available on the *Blood* website).

Mouse model

Mx1-Cre; Npm1$^{flox-cA/+}$ mice have been described previously.[19,20] Cre expression was induced in 8 to 10 weeks old *Mx1-Cre; Npm1*$^{flox-cA/+}$ mice by administration of polyinosinic:polycytidylic acid (catalog no. P1530; Sigma-Aldrich). Blood counts were calculated by a Scil Vet abc hematology analyzer. All mice were kept in a pathogen-free environment, and all procedures were performed according to the regulation of the UK Home office, under project license PP3797858, in accordance with the Animal Scientific Procedures Act 1986.

Proteomic analysis of preleukemic murine hematopoietic progenitors

A total of 7 *Npm1*$^{cA/+}$ and 5 control *Npm1*$^{+/+}$ mice were collected 8 weeks after polyinosinic:polycytidylic acid, and the bone marrow lineage-negative (lin$^-$) cells were subjected to proteomic analysis (supplemental Table 1). Sample preparation, mass spectrometry analysis, and data processing are described in detail in the supplemental Methods.

Proteomic and RNA expression analysis of samples from patients with AML

Experimental procedures and data sets can be found in Kramer et al.[22] *t* test was used to calculate *P* values for differences between the NPM1wt and NPM1c$^+$ AML groups, followed by multiple hypothesis correction using the Benjamini-Hochberg method.

Study of patient-derived *NPM1*-mutant AML cells

For patient-derived xenograft (PDX) studies, 1 × 10^6 cells of a luciferase-expressing *NPM1*-mutant AML PDX were injected IV into NOD.Cg-Prkdcscid Il2rgtm1Wjl/SzJ mice, and animals were treated with intraperitoneal ActD or vehicle from day 35 after transplantation and monitored for AML tumor volume and survival. Detailed experimental procedures are provided in the supplemental Methods.

NPM1-mutant normal karyotype AML cells were obtained from a 33-year-old man with the patient's informed consent as part of the Hémopathies Inserm Midi-Pyrénées collection (BB-0033-00060). According to French law, the Hémopathies Inserm Midi-Pyrénées collection has been declared to the Ministry of Higher Education and Research (DC 2008-307 collection 1) and a transfer agreement (AC 2008-129) was obtained after approbation by the Comité de Protection des Personnes Sud-Ouest et Outremer II (ethical committee). The study was performed in accordance with the Declaration of Helsinki.

Results

Npm1$^{cA/+}$ hematopoietic progenitors have reduced levels of ribosome biogenesis proteins

We collected bone marrow lineage-depleted (lin$^-$) hematopoietic stem/progenitor cells (HSPCs) 8 weeks after activation of the conditional *Npm1cA* allele in *Mx1-Cre; Npm1*$^{flox-cA/+}$ mice.[20] At that stage, the mice displayed normal hematological parameters and no signs of leukemia (supplemental Figure 1A-D), but the characteristic *Npm1c*-associated *HoxA* and *HoxB* gene upregulation was clearly evident in HSPCs (supplemental Figure 1E; supplemental Table 2). In line with this, *Npm1*$^{cA/+}$ HSPCs demonstrated enhanced serial replating in colony-forming unit assays, compared with their wild-type counterparts (supplemental Figure 1F-G).

To capture the global impact of isolated *Npm1c* mutations at the protein level, we performed tandem mass tag (TMT)-based quantitative proteomics in HSPCs from *Npm1*$^{cA/+}$ mutant (n = 7) vs *Npm1*$^{+/+}$ (n = 5) mice (Figure 1A). Of 7409 proteins detected overall, we found 58 high-confidence proteins whose abundance was significantly different (P_{adj} < .05) between *Npm1*$^{cA/+}$ and *Npm1*$^{+/+}$ HSPCs (Figure 1B; supplemental Table 3). Notably, NPM1 protein levels were found to be significantly reduced in *Npm1*$^{cA/+}$ mice. However, evaluation of the identified peptide spectra revealed that this was because the only NPM1-derived peptide detected was unique to the wild-type protein (amino acids 276-289). With no mutant-specific peptides identified, this resulted in an apparent reduction in NPM1 protein levels in heterozygous mice.

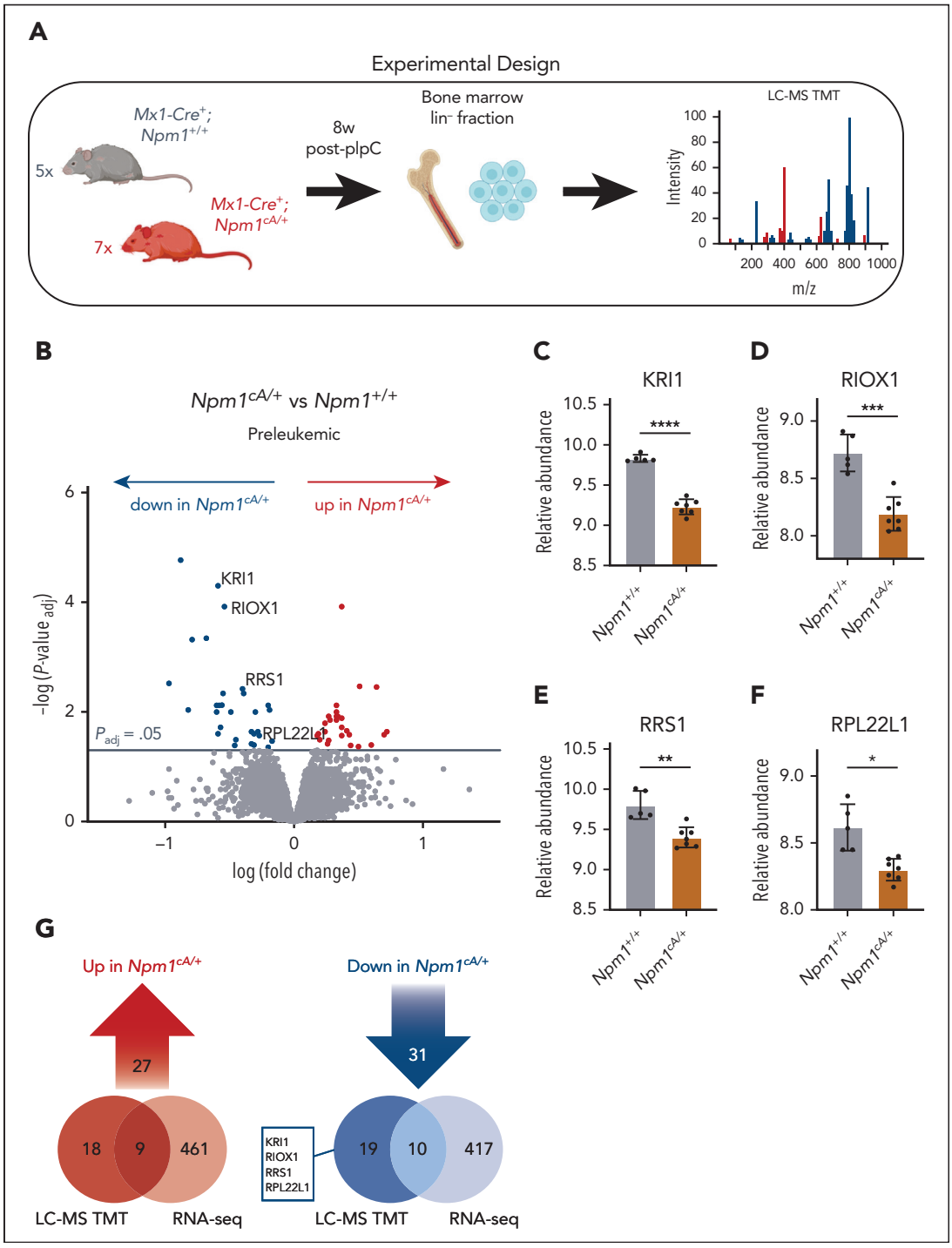

Figure 1. Reduced abundance of ribosomal proteins in *Npm1*$^{cA/+}$ hematopoietic progenitors. (A) Workflow for global quantitative proteomic study of lineage-negative (lin$^-$) bone marrow–derived hematopoietic progenitors using TMT. Preleukemic *Npm1*$^{cA/+}$ (n = 7) vs *Npm1*$^{+/+}$ (n = 5) murine hematopoietic progenitors were collected 8 weeks after *Mx1*-Cre induction with plpC. (B) Volcano plot revealing relative protein abundances in preleukemic *Npm1*$^{cA/+}$ vs *Npm1*$^{+/+}$ lin$^-$ progenitors. (C-F) Relative abundance of selected ribosome-related proteins in *Npm1*$^{cA/+}$ vs *Npm1*$^{+/+}$ lin$^-$ progenitors. (G) Overlap between messenger RNAs (RNA-seq) and proteins (LC-MS) that were significantly over- or under-expressed in preleukemic *Npm1*$^{cA/+}$ vs *Npm1*$^{+/+}$ lin$^-$ cells. Panel B, unpaired *t* test with multiple-hypothesis–testing correction (FDR; Benjamini-Hochberg). (C-F) Unpaired *t* test with multiple-hypothesis–testing correction (FDR; Benjamini-Hochberg). *$P \le .05$; **$P \le .01$; ***$P \le .001$; ****$P \le .0001$. Data represent n = 7 (*Npm1*$^{cA/+}$) or n = 5 (*Npm1*$^{+/+}$) biological replicates (mean ± SD). FDR, false discovery rate; LC-MS TMT, liquid chromatography mass spectrometry, tandem mass tagging; plpC, polyinosinic:polycytidylic acid. Panels A and G were created with BioRender.com. Vassiliou, G. (2025) https://BioRender.com/9tt8kww.

The top 3 proteins with the most significantly increased levels were the polyol pathway enzyme SORD (sorbitol dehydrogenase), the centrosomal protein CEP44 (centrosomal protein 44), and the F13A1 (coagulation factor XIII A chain) blood coagulation factor (supplemental Figure 2A-C). In addition, among proteins having increased abundance were several members of the Karyopherin family (supplemental Figure 2D), mirroring recent findings in human *NPM1c*-mutant AML.[22]

Interestingly, NPM1c$^+$ OCI-AML3 cells were found to be particularly sensitive to *KPNA2* knockout (DepMap[24,25]; supplemental Figure 2F-G).

Among the 31 proteins having decreased abundance in *Npm1*$^{cA/+}$ HSPCs, there were several ribosome-related proteins, including ribosome biogenesis factors and structural constituents of ribosomes.[7] Significantly depleted proteins included KRI1 (KRI1 homolog),[26] RIOX1 (ribosomal oxygenase 1),[27] RRS1 (ribosome biogenesis regulator 1 homolog),[28,29] and RPL22L1 (ribosomal protein L22 like 1)[30] (Figure 1C-F), none of which demonstrated reduction at the messenger RNA level (Figure 1G). Gene ontology term analysis of all depleted proteins (n = 270) among the top 500 differentially abundant proteins demonstrated enrichment for the preribosome and biological processes involving rRNA processing and ribosome biogenesis (supplemental Figure 3A; supplemental Table 4). Polysome profiling of whole bone marrow cells from *Npm1*$^{cA/+}$ and control *Npm1*$^{+/+}$ mice revealed no major differences, although there was a trend toward higher abundance for the 40S ribosomal subunit in the mutant cells (supplemental Figure 3B-E).

Ribosome biogenesis factors are depleted in human NPM1c$^+$ AML

To pinpoint which changes identified in NPM1c$^+$ preleukemic cells can also be detected after progression to AML, we evaluated recently reported TMT proteomics data from bone marrow samples of 44 patients with de novo AML, including 8 with NPM1c$^+$ AML.[22] By comparing protein levels between NPM1c$^+$ and NPM1wt AMLs, we identified only 11 significantly differentially abundant proteins (P_{adj} < .05), among which KRI1 was the most depleted (Figure 2A-B; supplemental Table 5). Importantly, gene ontology analysis of all depleted proteins (n = 191) among the top 500 differentially abundant proteins revealed an enrichment for ribosome biogenesis factors, rRNA processing enzymes, and maturation factors of rRNA precursors (supplemental Figure 4A; supplemental Table 6), similar to the murine preleukemic cells. RIOX1, RRS1, and RPL22L1, all of which were significantly depleted in preleukemic *Npm1*$^{cA/+}$ cells, also demonstrated reduced abundance in NPM1c$^+$ AML (Figure 2C-E), albeit without reaching significance after correcting for multiple testing. Other ribosome-related proteins that were depleted in NPM1c$^+$ AML included KRR1 (KRR1 small subunit processome component homolog), an important interactor of KRI1,[26] RPS9 (ribosomal protein S9), and RBIS (ribosomal biogenesis factor) (supplemental Figure 4B-D). Notably, none of the abovementioned candidates demonstrated downregulation in RNA-seq data from the same patients, suggesting that these genes/proteins are regulated posttranscriptionally (Figure 2F-I; supplemental Figure 4E-G). Finally, no significant differences were observed in the abundance of the abovementioned proteins between NPM1c$^+$, FLT3-ITD$^+$, and all other NPM1c$^+$ AMLs (supplemental Figure 4H), suggesting that these changes were not related to *FLT3-ITD*, the most common comutation of *NPM1c* in AML.

Preleukemic *Npm1*$^{cA/+}$ HSPCs demonstrate enhanced sensitivity to RNA pol I inhibitors

In light of the mislocalization of mutant and the reduced levels of NPM1wt, targeting ribosome homeostasis has been previously proposed as a therapeutic strategy against *NPM1*-mutant AML.[31-33] Our data suggest that, in addition to the reduced levels of NPM1wt in the nucleolus, mutant cells are depleted of several ribosome biogenesis factors. We hypothesized that this depletion creates a vulnerability that can be therapeutically exploited to specifically target mutant cells. To test this, we compared the responses of preleukemic *Npm1*$^{cA/+}$ vs control *Npm1*$^{+/+}$ HSPCs to drugs that modulate ribosome biogenesis, including ActD and other RNA pol I inhibitors. Indeed, we found that compared with *Npm1*$^{+/+}$ cells, preleukemic *Npm1*$^{cA/+}$ lin$^-$ cells were significantly more sensitive to ActD treatment (Figure 3A-C), particularly at lower concentrations where the drug effects are known to be on-target (supplemental Figure 5A).[34] Following treatment with low-dose ActD (1 nM), both mutant and wt HSPCs exhibited characteristic features of nucleolar stress, including a shift in nucleolar shape from irregular to round conformation (Figure 3D).[35,36] This suggests that both cell types activate a nucleolar stress response, although impact on survival is greater for NPM1c$^+$ cells. Nucleoplasmic dislocation of NPM1wt, another indicator of nucleolar stress,[33,36,37] was observed in preleukemic *Npm1*$^{cA/+}$ lin$^-$ cells treated with higher drug doses (5 nM) (supplemental Figure 5B). No DNA damage was observed in *Npm1*$^{cA/+}$ lin$^-$ cells after treatment with 2.5 nM ActD for 48 hours (supplemental Figure 5C).

To further test whether the preferential sensitivity of *Npm1*$^{cA/+}$ cells to ActD was due to RNA Pol I inhibition, and not due to off-target effects, we then tested BMH-21 and CX-5461, 2 more recently developed small-molecule inhibitors with different modes of RNA pol I inhibition.[38-40] Similarly to ActD, we found that *Npm1*$^{cA/+}$ HSPCs were significantly more sensitive to both agents compared with wild-type *Npm1*$^{+/+}$ cells (Figure 3E-F; supplemental Figure 5D-G). Although off-target effects cannot be entirely excluded, the consistent phenotype observed across the 3 chemically distinct compounds suggests that *Npm1c* specificity is primarily driven by on-target RNA pol I inhibition. By contrast, we did not observe differential sensitivity between *Npm1*$^{cA/+}$ and *Npm1*$^{+/+}$ HSPCs to cycloheximide, a drug that inhibits translational elongation (Figure 3G).

Single-agent ActD inhibits expansion of an *NPM1*-mutant AML PDX

To investigate the effects of ActD treatment in vivo using a clinically relevant AML model, we used a luciferase-expressing *NPM1*-mutant PDX harboring *DNMT3A R882H*, *FLT3-ITD*, and *RAD21 R146G* comutations. One million NPM1c$^+$ AML PDX cells were injected IV into 12 NOD.Cg-Prkdcscid Il2rgtm1Wjl/SzJ mice (Figure 4A; supplemental Figure 6A). After 35 days, mice were allocated into 2 groups of similar AML burden (Figure 4B) to receive ActD (0.1 mg kg^{-1}) or vehicle twice weekly for 5 weeks. Repeat bioluminescent imaging revealed a significant reduction of AML burden in ActD-treated animals at 45 and 58 days after IV injection (Figure 4C-E). Dosing was reduced to 0.06 mg kg^{-1} once weekly for another 3 weeks, and animals were monitored until they developed leukemia symptoms. ActD-treated animals had a significantly longer survival at 90 days (P = .031), but this became nonsignificant soon after stopping the treatment and until the end of the study (median survival ActD 84.5 days vs vehicle 99 days) (supplemental

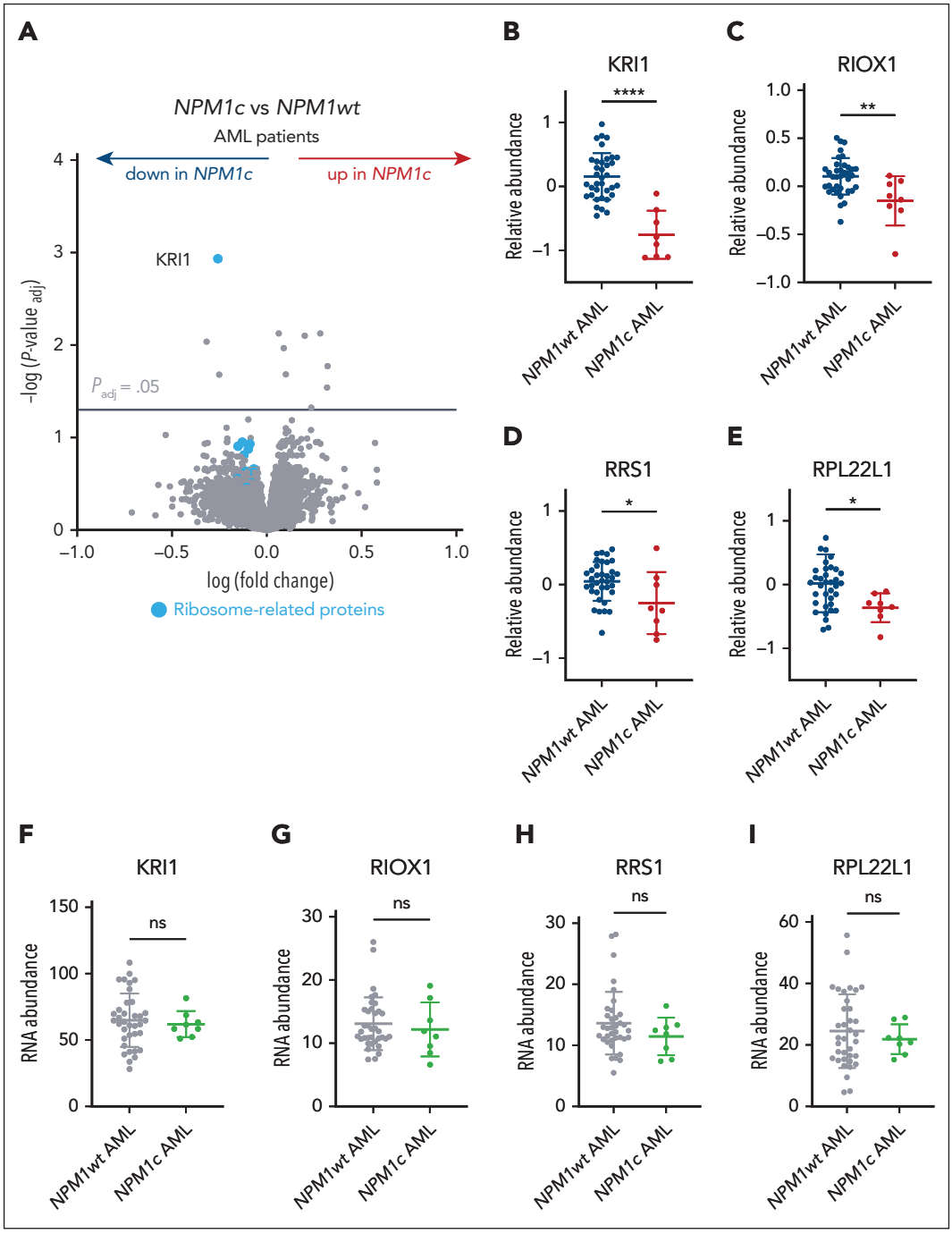

Figure 2. Depletion of ribosome processing factors in human NPM1c$^+$ AML. (A) Volcano plot of protein abundance in bone marrow samples from NPM1c$^+$ (n = 8) vs NPM1wt (n = 36) human de novo AMLs.[22] (B-I) Relative protein (B-E) or RNA abundance (F-I) of selected ribosome-related candidates in NPM1c$^+$ (n = 8) vs NPM1wt (n = 36) AML patients (mean ± SD). Panel A, unpaired *t* test with multiple-hypothesis–testing correction (FDR, Benjamini-Hochberg method). (B-I) Unpaired *t* test was used to calculate *P* values between groups. *$P \leq .05$; **$P \leq .01$; ****$P \leq .0001$. ns, nonsignificant. Data available in Kramer et al.[22]

Figure 6B). Notably, at collection, ActD-treated mice exhibited milder AML-related pathological findings, including significantly smaller spleens, lower white blood cell, and higher platelet counts (Figures 4F-H). The antileukemic effect of ActD was also confirmed by the significant reduction of circulating human CD45+ AML cells in the blood (Figure 4I) and trends toward lower levels in the bone marrow and spleen (supplemental Figure 6C-D). Overall, these data reveal that single-agent ActD has antileukemic activity in vivo against human *NPM1*-mutant AML. Nonetheless, further studies will be needed to assess the selectivity of this treatment for patients with NPM1c$^+$ AML vs patients with NPM1wt AML.

ActD potentiates the effects of venetoclax against preleukemic and leukemic NPM1c$^+$ cells

Because venetoclax has become the standard of care for the older/unfit patients with AML and is particularly effective

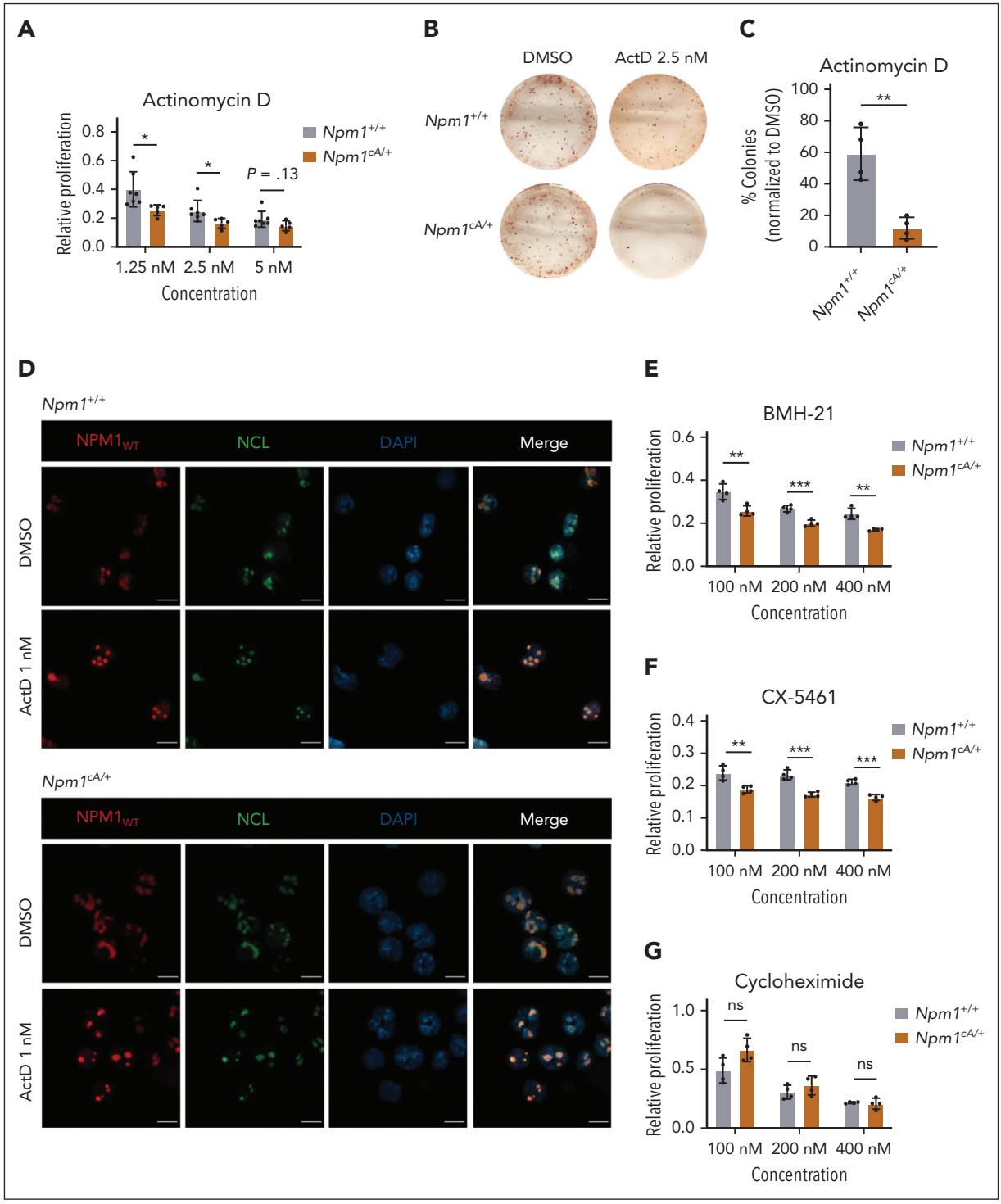

Figure 3. Preleukemic *Npm1*$^{cA/+}$ cells demonstrate enhanced sensitivity to RNA pol I inhibitors. (A) Relative proliferation of preleukemic *Npm1*$^{cA/+}$ vs *Npm1*$^{+/+}$ lin$^-$ cells after 4 days of treatment with ActD at the indicated doses (MTS assay). (B) Representative CFU assays from preleukemic *Npm1*$^{cA/+}$ vs *Npm1*$^{+/+}$ lin$^-$ cells after 24 hours pretreatment with 2.5 nM ActD. (C) Total number of colonies in CFU assays of preleukemic *Npm1*$^{cA/+}$ vs *Npm1*$^{+/+}$ lin$^-$ cells after 24 h pretreatment with 2.5 nM of ActD. (D) Nucleolar morphology of *Npm1*$^{+/+}$ (top panel) or *Npm1*$^{cA/+}$ (bottom panel) lin$^-$ cells after treatment with 1 nM ActD for 18 hours, highlighted using fluorescent staining for wild-type NPM1 (NPM1$_{WT}$) and nucleolin (NCL) (scale, 10 μm). (E-G) Relative proliferation of preleukemic *Npm1*$^{cA/+}$ vs *Npm1*$^{+/+}$ lin$^-$ cells after 4 days of treatment with BMH-21 (E), CX-5461 (F), or cycloheximide (G) at the indicated doses (MTS assay). (A,C,E-G) Unpaired *t* test was used to calculate *P* values between groups. *$P \leq .05$; **$P \leq .01$; ***$P \leq .001$. (A,E-G) Absorbance values were normalized to DMSO-treated cells. Data represent 4 to 7 biological replicates per group (mean ± SD). (C) Values represent 4 biological replicates per group. (D) Representative example from 1 of 2 to 4 biological replicates. DAPI, 4′,6-diamidino-2-phenylindole.

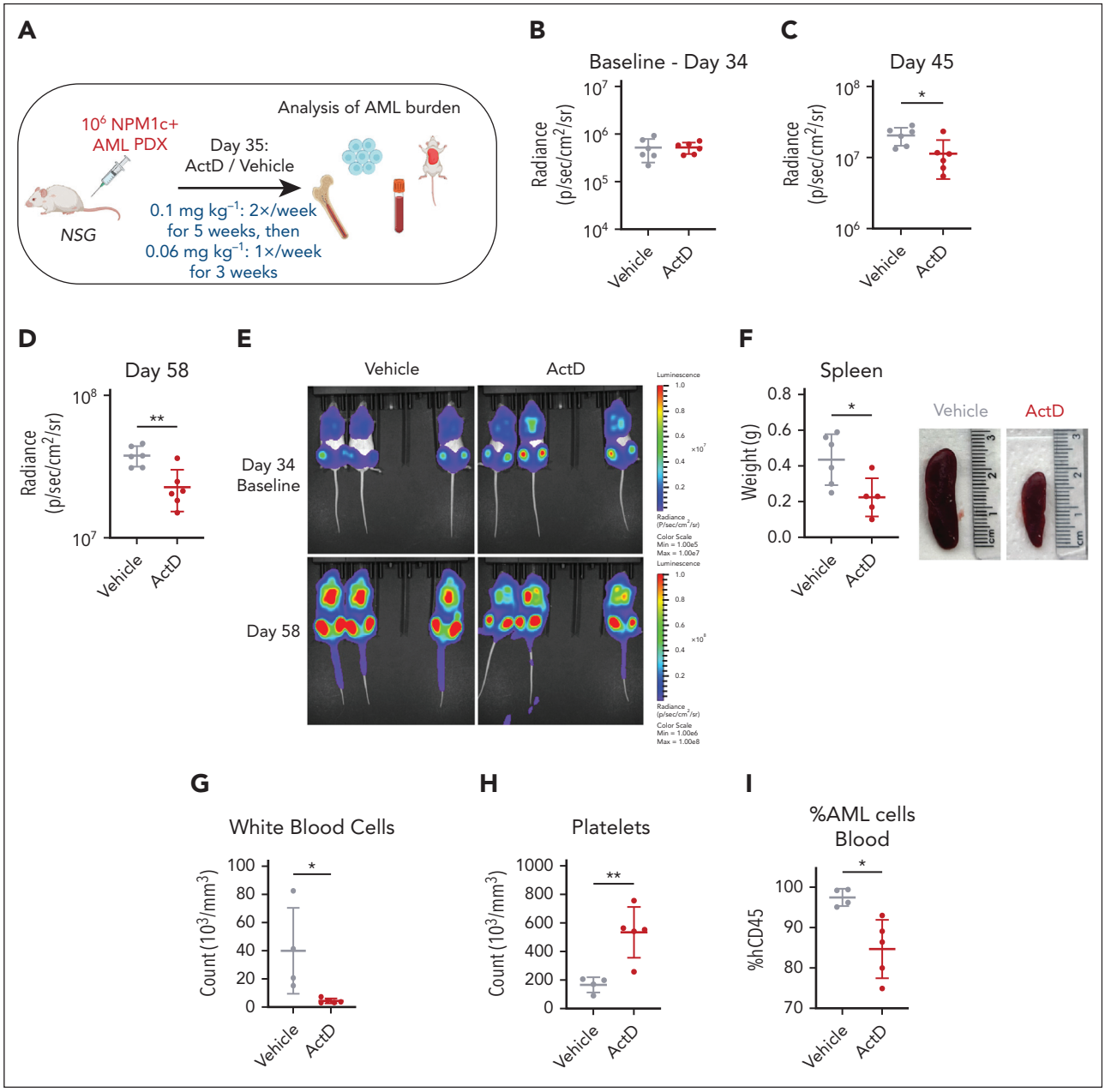

Figure 4. Actinomycin D reduces AML burden in a xenograft model. (A) Schematic representation of PDX experiment. Mice transplanted with 10^6 luciferase-expressing NPM1c$^+$ AML PDX cells were treated with 0.1 mg kg^{-1} ActD or vehicle twice weekly for 5 weeks, followed by treatment with 0.06 mg kg^{-1} ActD or vehicle once weekly for another 3 weeks. Leukemia burden was monitored by bioluminescence imaging and quantified in tissues after animal collection. (B-D) Bioluminescence radiance on day 34 (baseline) (B), day 45 (C), and day 58 (D) in ActD vs vehicle-treated animals. (E) Bioluminescence imaging of animals treated with ActD vs vehicle at indicated time points. (F) Spleen weights and representative spleen pictures in ActD vs vehicle-treated animals. (G-H) Counts of white blood cells (G) and platelets (H) in ActD vs vehicle-treated animals. (I) Percentage of cells expressing human CD45 (hCD45) of total CD45 in blood in ActD vs vehicle-treated animals. (C-D,F-I) Unpaired *t* test was used to calculate *P* values between groups. **P* ≤ .05; ***P* ≤ .01. Data represent 4 to 6 biological replicates per group (those with available tissues on disease presentation) (mean ± SD). Panel A was created with BioRender.com. Vassiliou, G. (2025) https://BioRender.com/9tt8kww.

against *NPM1*-mutant AML,[41,42] we next wanted to evaluate whether the ActD-venetoclax combination could synergistically suppress the growth of NPM1c$^+$ hematopoietic cells. We found that doses of ActD or venetoclax that had mild effects on cell proliferation in isolation significantly inhibited the growth of preleukemic *Npm1*$^{cA/+}$ hematopoietic progenitors in liquid culture when combined (Figure 5A). Moreover, the combination of ActD and venetoclax synergistically reduced the number of total colony-forming unit colonies in semisolid media at doses that had minimal anticlonogenic effect when each drug was used in isolation (Figure 5B-C).

In a similar fashion, ActD treatment synergistically enhanced the antileukemic effects of venetoclax in murine *Npm1*$^{cA/+}$; *Flt3*$^{ITD/+}$ AML cells (Figure 4D). In the same model, high zero interaction potency synergistic scores were obtained in 3-(4,5-dimethylthiazol-2-yl)-5-(3-carboxymethoxyphenyl)-2-(4-sulfophenyl)-2H-tetrazolium (MTS) proliferation assays when venetoclax was

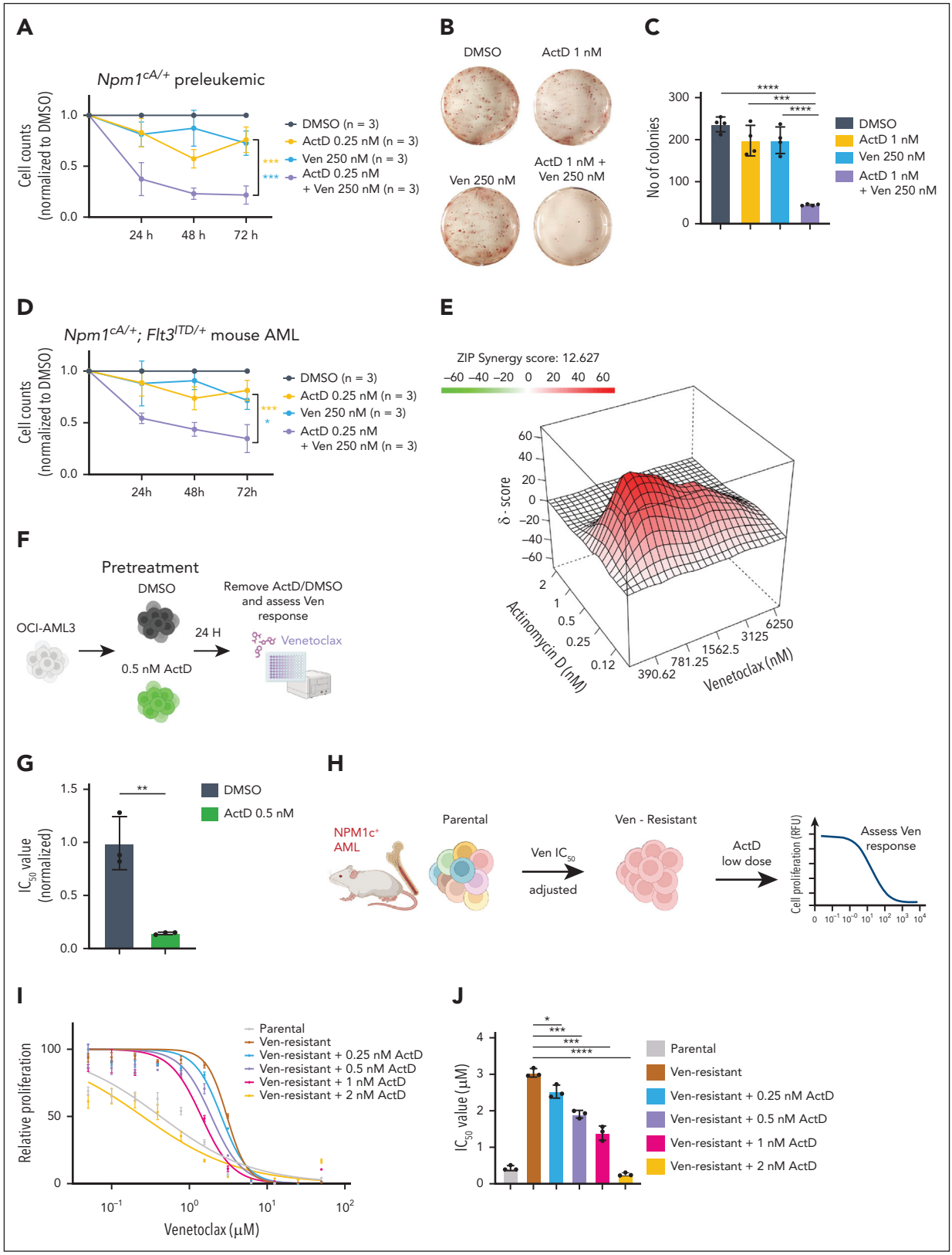

Figure 5. Actinomycin D enhances cytotoxicity and reverses resistance to Ven in NPM1c$^+$ preleukemic and leukemic cells. (A) Counts of preleukemic *Npm1*$^{cA/+}$ lin$^-$ cells treated with DMSO, ActD, venetoclax (Ven), or a combination (mean ± SD, n = 3 independent experiments). (B) Representative CFU assays of preleukemic *Npm1*$^{cA/+}$ lin$^-$ cells treated with DMSO, ActD, Ven, or a combination. (C) Total CFU colony numbers of preleukemic *Npm1*$^{cA/+}$ lin$^-$ cells treated with DMSO, ActD, Ven, or a combination (n = 2 biological replicates, each performed in duplicate). (D) Counts of murine *Npm1*$^{cA/+}$; *Flt3*$^{ITD/+}$AML cells treated with DMSO, ActD, Ven, or a combination (mean ± SD, n = 3 independent experiments). (E) Representative synergy plot revealing the interaction between ActD and Ven in inhibiting the proliferation of murine *Npm1*$^{cA/+}$; *Flt3*$^{ITD/+}$AML cells after 4 days of drug incubation (MTS assay) (representative examples from 1 of 3 independent experiments). (F) OCI-AML3 cells were pretreated with 0.5 nM ActD vs

combined with low concentrations of ActD (Figure 5E; supplemental Figure 7A).

Low-dose ActD treatment resensitizes resistant *NPM1*-mutant AML cells to venetoclax

NPM1c-mutant OCI-AML3 cells carry biallelic loss-of-function *BAX* mutations and are resistant to venetoclax (supplemental Figure 7B-C). We pretreated OCI-AML3 cells for 24 hours with low-dose ActD (0.5 nM), a concentration that did not affect cell viability (supplemental Figure 7D). We, then, removed ActD and exposed the pretreated cells to a range of doses of venetoclax (Figure 5F). We found that ActD pretreated OCI-AML3 were significantly more sensitive to venetoclax compared with dimethyl sulfoxide (DMSO)-pretreated cells, with a dramatic fivefold reduction in 50% inhibitory concentration (IC_{50}) (Figure 5G; supplemental Figure 7E). In addition, Annexin V staining demonstrated a significant increase in apoptosis induction in *NPM1*-mutant cells after combination treatment with low-dose ActD and venetoclax (supplemental Figure 7F).

To test whether this observation held true for acquired venetoclax resistance outside immortalized cell lines, we turned to our *Sleeping Beauty* transposon-driven NPM1c$^+$ AML model.[20] In brief, we exposed murine NPM1c$^+$ AML cells harboring active (jumping) transposons to gradually increasing doses of venetoclax, until they developed resistance. The derivative resistant AML cells displayed a 4 to 7 times higher IC_{50} value for venetoclax compared with the parental cells. However, as with the OCI-AML3 cells, pretreatment with low concentration of ActD restored their sensitivity to venetoclax in a dose-dependent manner (Figure 5H-J; supplemental Figure 7G-H).

NPM1c$^+$ AML cells are preferentially sensitive to inhibition of the 40S maturation pathway

Ribosome biogenesis is a highly orchestrated process involving more than 200 different factors.[7] ActD targets the first step in the process, namely transcription of the polycistronic 47S pre-rRNA precursor, but in higher concentrations can have pleiotropic effects and associated toxicities.[38] Thus, we next wanted to explore whether ribosome biosynthesis could be targeted in NPM1c$^+$ AML cells in alternative ways, by inhibiting specific ribosome-related factors.

To investigate this, we started by evaluating the DepMap database, which contains CRIPSR knockout data for hundreds of different cancer cell lines.[24,25] We isolated the top 500 preferentially essential genes for OCI-AML3 (the only NPM1c$^+$ cell line in the database), whose knockout is more detrimental to this cell line vs other cancer cell lines. From this list, we selected all genes with a known role in ribosome biogenesis, including ribosomal components and factors involved in rRNA transcription, modification, assembly, and maturation (Figure 6A). Candidates recovered in the list included NPM1 itself, the rDNA transcription factor UBTF, NOP56, which is a core component of box C/D small nucleolar ribonucleoprotein particles, and RPS6KA1, a member of the RSK family of kinases that is involved in the phosphorylation of RPS6 and is druggable[43,44] (supplemental Figure 8A-F).

Notably, among the list of preferentially essential genes for OCI-AML3 cells, we found an enrichment for factors that are involved in related steps of the 40S ribosome maturation pathway, including the ribosome assembly factors BYSL, TSR1, and TSR3. BYSL and TSR1 bind early 40S precursors in the nucleoplasm and are exported bound to the pre-40S subunit to the cytoplasm, where TSR3 is then recruited for the final stages of maturation.[7] Loss of any of these 3 factors had a strong, preferential antileukemic effect against OCI-AML3 cells, compared with a panel of 37 different AML cell lines (Figure 6B-D; supplemental Figure 9A).

TSR3 is an aminocarboxypropyl (acp) transferase responsible for the hypermodification of the 18S rRNA during late 40S maturation steps in the eukaryotic cytoplasm. Unlike *BYSL* and *TSR1* which are common essential genes,[24,25] *TSR3* is not broadly essential for cell survival,[45,46] making it an attractive therapeutic target. Notably, an independent CRISPR knockout screen also identified *TSR3* as a specific vulnerability of OCI-AML3 cells, but not of the other 4 different AML cell lines tested (OCI-AML2, MOLM-13, HL-60, and MV-4-11)[23] (Figure 6E). We decided to focus on TSR3 for validation studies for the following reasons: (1) specificity against NPM1c$^+$ AML; (2) cross-validation in 2 independent CRISPR screens[23-25]; (3) participation in the 40S subunit maturation, disruption of which is particularly detrimental for NPM1c$^+$ cells; (4) nonessential function in normal cells[45,46]; and (5) potentially druggable profile.[46] We confirmed that *TSR3* knockout inhibits the growth of OCI-AML3 cells (Figure 6F) but has little or no effect on the proliferation of NPM1wt cell lines (supplemental Figure 9B). In addition, *Tsr3* targeting reduced the proliferation of murine *Npm1*$^{cA/+}$; *Flt3*$^{ITD/+}$ leukemic cells (Figure 6G), but not of murine AML cells driven by *Flt3*$^{ITD/+}$ and oncogenic *MLL* gene fusions (supplemental Figure 9C). Finally, *Tsr3* knockout did not affect the growth of the non-leukemic murine hematopoietic progenitor line 32D (Figure 6H).

Upregulation of p53 targets and induction of apoptosis in *TSR3*-depleted NPM1c$^+$ AML cells

Next, we wanted to investigate the effects of *TSR3* knockout on NPM1c$^+$ AML cells. RNA-seq analysis revealed the upregulation of many direct p53 target genes, including *CYFIP2*, *CDKN1A*, and *PHLDA3*, shortly after *TSR3* depletion (Figure 7A; supplemental Table 7). We performed gene set enrichment analysis of RNA-seq from *TSR3*-depleted OCI-AML3 cells and found an enrichment for genes involved in apoptosis and a depletion of E2F targets and G2M checkpoint genes (supplemental Figure 10A-C). Conversely, no apoptosis or cell cycle-related gene sets were significantly altered in

Figure 5 (continued) DMSO for 24 hours and then tested for sensitivity to venetoclax. (G) IC_{50} values of DMSO or ActD pretreated OCI-AML3 cells after 4 days of incubation with Ven at the indicated doses (MTS assay). (H) Outline of approach to generate Ven-resistant murine *Npm1c*-mutant AML cells by treatment with escalating concentrations of Ven. Ven-resistant cells were then pretreated with ActD for 24 hours and their sensitivity to Ven was assessed using the MTS assay. (I) Relative proliferation of DMSO or ActD pretreated murine NPM1c$^+$ AML cells after 4 days incubation with Ven at the indicated doses. Absorbance values were normalized to DMSO-treated cells (mean ± SD, data from 1 of 2 biological replicates, performed in triplicate). (J) IC_{50} values of DMSO or ActD pretreated murine NPM1c$^+$ AML cells after 4 days of incubation with Ven (mean ± SD, data from 1 of 2 biological replicates, performed in triplicate). (A,C-D,G,J) *t* test was used to calculate *P* values between groups. *$P \le .05$; **$P \le .01$; ***$P \le .001$; ****$P \le .0001$. ZIP, zero interaction potency. Panels F and H were created with BioRender.com. Vassiliou, G. (2025) https://BioRender.com/9tt8kww.

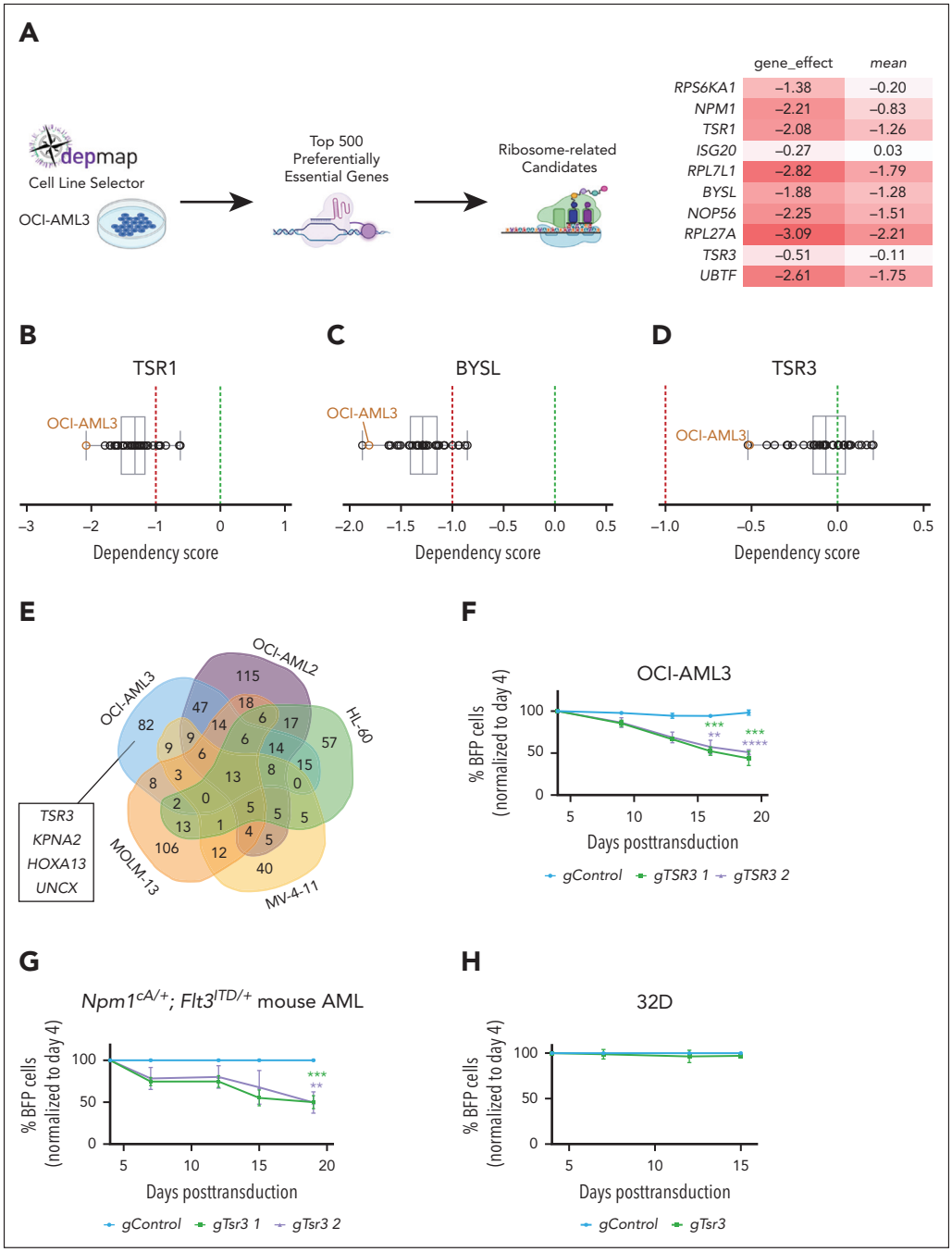

Figure 6. NPM1c$^+$ AML cells are preferentially sensitive to the inhibition of *TSR3* and related ribosome biogenesis factors. (A) Analysis of DepMap data was used to identify the top 500 preferentially essential genes for the OCI-AML3 cell line. Of these, candidates with an established role in ribosome biogenesis are highlighted (right). The "gene_effect" represents the dependency score of each candidate for OCI-AML3 cells, where a score of 0 indicates that the gene is not essential, whereas a score of −1 corresponds to the median of all common essential genes in the database. The mean represents the mean gene effect across all cancer cell lines in the database. (B-D) Differential dependency of 37 AML cell lines to CRISPR knockout of *TSR1* (B), *BYSL* (C), or *TSR3* (D) according to DepMap. (E) Venn diagram of gene dropouts in a CRISPR screen with 5 AML cell lines (OCI-AML3, OCI-AML2, MOLM-13, HL-60, and MV-4-11).[23] (F-H) Relative proliferation of OCI-AML3 (F), murine *Npm1*$^{cA/+}$; *Flt3*$^{ITD/+}$AML (G), or nonleukemic 32D (H) cells on knockout of *TSR3* as measured by a competitive proliferation assay of gRNA-BFP positive (BFP$^+$) transduced cells vs untransduced BFP negative (BFP$^-$) cells in 15 to 18 days. BFP percentage was normalized to the day 4 reading and for panel G to the "gControl" (mean ± SD, n = 3 independent experiments). (F-G) *t* test was used to calculate *P* values between groups. $^{**}P \le .01$; $^{***}P \le .001$; $^{****}P \le .0001$. (A-D) CRISPR scores originate from the DepMap Public 23Q2+Score, Chronos data set.[24,25] Panel A was created with BioRender.com. Vassiliou, G. (2025) https://BioRender.com/9tt8kww.

TSR3-depleted OCI-AML2 cells (NPM1wt) at the same time point (supplemental Figure 10D-F).

Reflecting these findings, *TSR3* knockout increased apoptosis in OCI-AML3 cells and murine *Npm1*$^{cA/+}$; *Flt3*$^{ITD/+}$ leukemia cells (Figure 7B-7D; supplemental Figure 10G-I), while also affecting cell cycle distribution (Figure 7E; supplemental Figure 10J). In contrast, we did not observe any significant alterations in apoptosis or the cell cycle distribution on *TSR3* knockout in OCI-AML2 cells (supplemental Figure 10K-M).

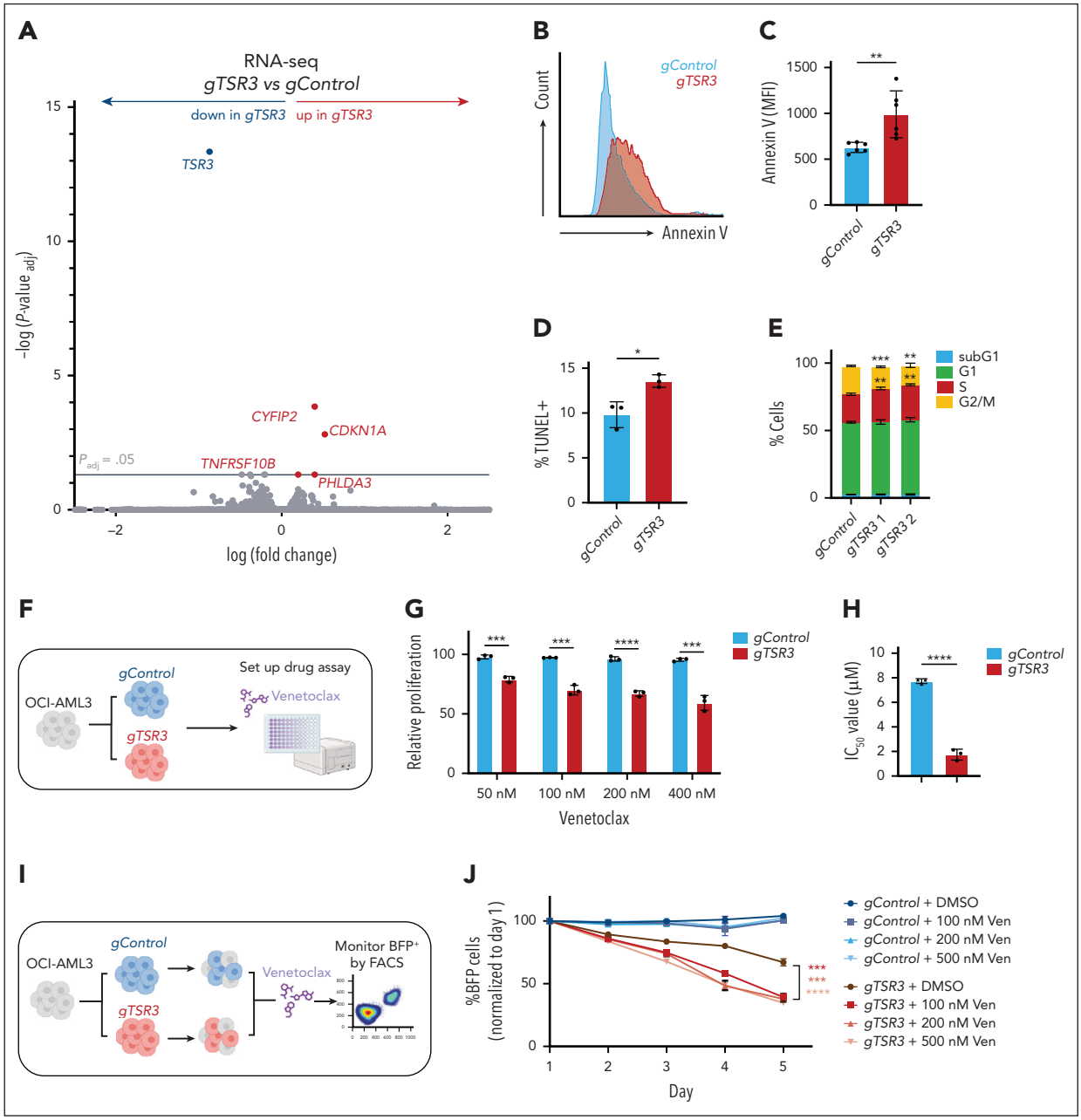

Figure 7. *TSR3* knockout activates a p53-dependent response and resensitizes resistant NPM1c$^+$ AML cells to Ven. (A) Volcano plot revealing differentially expressed genes in OCI-AML3 cells transduced with a *TSR3* gRNA (*gTSR3*) vs a nontargeting control gRNA (*gControl*). (B) Representative histogram plot of Annexin V staining in g*TSR3* vs *gControl*-transduced OCI-AML3 cells. (C) Annexin V staining, (D) TUNEL staining, and (E) cell cycle distribution in g*TSR3* vs *gControl*-transduced OCI-AML3 cells. (F) Schematic representation of the OCI-AML3 presensitization experiment. OCI-AML3 cells were transduced with *gTSR3* or *gControl* and their response to venetoclax (Ven) was assessed using the MTS assay. (G) Proliferation of g*TSR3* vs *gControl*-transduced OCI-AML3 cells after 4 days of incubation with Ven at the indicated doses (MTS assay). (H) IC_{50} values of g*TSR3* vs *gControl*-transduced OCI-AML3 cells after 4 days of incubation with Ven (MTS assay). (I) Schematic representation of resensitization experiment using OCI-AML3 cells. Cells were transduced with BFP-expressing *gTSR3* or *gControl* and were mixed with BFP-negative untransduced cells. Next, they were exposed to Ven and the BFP$^+$ percentage was monitored for a course of 5 days by flow cytometry. (J) Percentage of BFP$^+$ *gTSR3* or *gControl*-transduced cells on treatment with Ven at the indicated doses. BFP percentage was normalized to the reading of day 1. (A) Unpaired *t* test with multiple-hypothesis–testing correction (FDR, Benjamini-Hochberg method). (C-E,G-H,J) *t* test was used to calculate *P* values between groups. **P* ≤ .05; ***P* ≤ .01; ****P* ≤ .001; *****P* ≤ .0001. Data represent 3 to 6 independent experiments (mean ± SD). (G-H) Absorbance values were normalized to DMSO-treated cells. Data represent 3 independent experiments (mean ± SD). MFI, mean fluorescence intensity. Panels F and I were created with BioRender.com. Vassiliou, G. (2025) https://BioRender.com/9tt8kww.

TSR3 depletion resensitizes resistant NPM1c$^+$ AML cells to venetoclax

Finally, we wanted to investigate whether *TSR3* depletion could restore venetoclax sensitivity of resistant NPM1c$^+$ leukemia cells, as found with low-dose ActD treatment. For this, we knocked out *TSR3* in OCI-AML3 cells and reassessed response to venetoclax (Figure 7F). Strikingly, we observed that on *TSR3* depletion, OCI-AML3 cells responded to concentrations as low as 50 nM, whereas control guide RNA (gRNA)-transduced cells required 100 to 200 times higher concentrations to display a similar effect (Figure 7G; supplemental Figure 11A-B). Overall, IC_{50} was four and a half-fold lower in *TSR3*-depleted compared

with control OCI-AML3 cells (Figure 7H; supplemental Figure 11C).

Next, we mixed BFP-expressing control gRNA and *TSR3* gRNA-transduced OCI-AML3 cells with nontransduced cells and treated with increasing venetoclax concentrations for a course of 5 days, while also monitoring the gRNA abundance using flow cytometry (Figure 7I). As expected, control gRNA-transduced cells demonstrated no decreased survival in the evaluated concentrations. In contrast, *gTSR3*-transduced cells demonstrated decreased survival that was also reduced on venetoclax treatment, further revealing the selective sensitivity of the *TSR3*-depleted cell population (Figure 7J; supplemental Figure 11D-G).

Discussion

NPM1c mutations are found in 30% of all AML cases.[13] Yet, despite some recent advances in understanding their molecular consequences,[47,48] current therapeutic outcomes remain suboptimal, highlighting the need for new effective treatments.[18] In this study, we identified *NPM1c*-induced proteomic changes and investigated their therapeutic potential. The use of a faithful conditional knockin mouse model allowed us to study the proteomic effects of *NPM1c* mutations in isolation, by overcoming the confounding effects of different comutations[19] or other sources of biological variation, including potential in vitro adaptive changes in transformed cell lines. This enabled us to establish a direct connection between the mutated NPM1c protein and observed phenotypes.

Our findings revealed that levels of many proteins involved in ribosome biogenesis are significantly reduced in NPM1c$^+$ cells, without significant changes in expression of their cognate messenger RNAs (RNA-seq), in keeping with altered post-transcriptional regulation. This downregulation could be either directly or indirectly triggered by the reduced levels of NPM1wt in mutant cells, although the precise mechanisms involved require further investigation. Potential scenarios include the following: (1) the interaction of NPM1wt with rRNA and ribosome biogenesis factors may stabilize them, with loss of this interaction in the mutant cells leading to protein degradation and (2) NPM1 haploinsufficiency may alter the availability of its chaperone partners or disrupt the structural organization of the nucleolus,[9,10] affecting interactions, levels, and stability of ribosome biogenesis factors. Interestingly, the altered nucleolar structure was recently found to be detectable by holotomography.[49] On the basis of the observed depletion of ribosome biogenesis factors, we hypothesized that targeting nucleolar homeostasis may selectively affect NPM1c$^+$ cells. Indeed, *NPM1*-mutant cells were selectively more sensitive to multiple RNA pol I inhibitors (ActD, CX-5461, and BMH-21) but displayed no differential response to translation inhibitors such as cycloheximide.

Importantly, reduced ribosomal factor levels are also evident after leukemia development, providing a rationale for reevaluating the concept of targeting ribosome biogenesis in NPM1c$^+$ AML, as first suggested and tested by Falini et al.[31,32] More recently, Gionfriddo et al[33] revealed that ActD could induce complete remission in patients with relapsed/refractory *NPM1*-mutant AML, with evidence that the treatment initiated a nucleolar stress response. Interestingly, Wu et al[50] discovered an additional effect of ActD in the mitochondria which contributed to its antileukemic effects.

In the second part of this study, we explored whether specific ribosome biogenesis factors can be targeted in *NPM1*-mutant leukemic cells. Using DepMap[24,25] and another independent genome-wide AML CRISPR screen,[23] we identified *TSR3*, a gene whose knockout preferentially reduced the proliferation of NPM1c$^+$ AML cells. TSR3 acts at the late cytoplasmic stages of the 40S ribosome maturation and is responsible for introducing the N1-methyl-N3-aminocarboxypropylpseudouridine ($m^1acp^3\Psi$) mark on 18S rRNA.[46] Interestingly, loss of the $m^1acp^3\Psi$ is a common event in cancer,[45] though it is unclear whether this loss confers a growth advantage or is simply a byproduct of the high ribosome production rates in cancer cells.

Currently, the mechanism underlying the dependency of NPM1c$^+$ AML on TSR3 is poorly understood, and it remains uncertain whether it relates to its enzymatic activity. The significantly reduced levels of the ribosome factors KRI1 and its interactor KRR1, both of which are acting upstream of TSR3 in 40S maturation,[7] could provide a potential link to explain this vulnerability. In this model, *TSR3* knockout, similarly to RNA pol I inhibition, could be exacerbating an already impaired ribosome biogenesis process in NPM1c$^+$ AML, lowering the threshold for p53 activation and leading to apoptosis.

Notably, both low-dose ActD treatments and *TSR3* knockout synergized with venetoclax and displayed the ability to induce at least partial resensitization in *NPM1*-mutant, venetoclax-resistant AML models. Previous studies have revealed that nucleolar stress, such as that caused by RNA pol I inhibition, leads to the diffusion of ribosomal proteins into the nucleoplasm, where they bind and sequester MDM2, resulting in p53 stabilization and upregulation of key apoptotic genes.[35,51-53] In addition, induction of p53-driven apoptosis was demonstrated in ActD-treated *NPM1*-mutant AML cells.[33] In line with these findings, our RNA-seq analysis of *TSR3*-depleted NPM1c$^+$ cells revealed the upregulation of direct p53 targets, including *CDKN1A* (p21), and an enrichment for genes involved in apoptosis. Importantly, p53 and the apoptotic response network have a central role in controlling sensitivity to venetoclax.[54,55] Taken together, these data suggest that activation of p53 and its targets by ActD or *TSR3* knockout works synergistically with BCL-2 inhibition (venetoclax) to promote apoptosis in *NPM1*-mutant AML cells.

Overall, our findings lead us to propose that acquisition of *NPM1c* and the accompanying loss of 1 *NPM1wt* allele result in the posttranscriptional depletion of multiple players involved in ribosome biogenesis, a consequence that can be exploited therapeutically to target *NPM1*-mutant AML cells (supplemental Figure 12).

Acknowledgments

The authors thank the Cancer Research UK Cambridge Institute Proteomics team, the Cambridge Biomedical Research Centre Phenotyping Hub, the Anne McLaren Biomedical Research Facility (especially Charlotte Townend), and the Cambridge Stem Cell Institute Genomics facility and Imaging facility (especially James Boyd) for providing expert technical assistance and support for our research project.

This work was funded by grants from Cancer Research UK (C22324/A24482) and AstraZeneca (G113590). G.S.V. is supported by a Cancer Research UK Senior Cancer Fellowship (C22324/A23015), and work in his laboratory is also funded by the European Research Council, Leukemia and Lymphoma Society, Rising Tide Foundation for Clinical Cancer Research, Kay Kendall Leukaemia Fund, Blood Cancer UK, and Wellcome Trust. A.D. is supported by Cancer Research UK (C22324/A24482) and AstraZeneca (G113590). K.T., E.Y., and M.E. are supported by Wellcome Trust (grants RG94424, RG83195, RG106133, and RG127005) and UKRI Medical Research Council (grant RG83195). K.T. and M.E. are supported by Leukaemia UK (grants 2020/JGF/004 and 2022/FuF/001). E.Y. is supported by a Leukaemia UK John Goldman Fellowship (2024/JGF/009). Work in the laboratory of A.J.W. is supported by Cancer Research UK (DRCNPG-Jun24/100002), UK Medical Research Council (MR/T012412/1), European Cooperation in Science and Technology, Action Translacore (CA21154), Blood Cancer UK (21002), Rosetrees Trust (PGL22/100032), Isaac Newton Trust (G125517), and Addenbrookes Charitable Trust (900426). J.-E.S. was supported by the Programme Investissement d'Avenir Projets de Recherche et Développement Structurants Pour la Compétitivité (Initiative de Modèles Innovants) and the Laboratoire d'Excellence Toulouse Cancer (TOUCAN; contract ANR11-LABEX). A. Sahal was a fellow from the European Regional Development Fund through the Interreg V-A Spain–France–Andorra (Programa Interreg España-Francia-Andorra) program, project PROTEOblood (EFA360/19; J.-E.S.).

Authorship

Contribution: G.S.V. conceived and supervised the study; G.S.V. and A.D. designed the experimental plan; A.D. carried out most of the experiments with help from R.W.; M. Gozdecka contributed to experimental design and provided scientific expertise; the in vivo patient-derived xenograft (PDX) experiment was performed with the help from G.G. (study design, animal procedures, imaging), R.A. (animal procedures, animal collection), and G.S.V. (intravenous injections); M.E. contributed to immunofluorescence imaging and animal collection and processing; M. Gu performed bioinformatic analysis and data deposition for the RNA sequencing experiments; primary AML characterization, sample collection, and PDX generation were carried out by C.R. (clinician), V.M.-D.M. (biobanking), F.V. (diagnosis), A. Sahal (PDX generation), B.V. (passaging and introduction of luciferase reporter), and I.J. and J.-E.S. (supervision); E.K.P., A. Sawle, and C.D'S. performed, analyzed, and provided scientific expertise for the preleukemic tandem mass tag proteomics experiment; E.Y., M.D., X.L., J. Russell, and J. Rak contributed to animal collection and processing; C.H. performed polysome profiling; I.J., J.-E.S., K.T., B.J.P.H., A.J.W., and O.T. provided scientific expertise; and G.S.V. and A.D. prepared the manuscript with help from all authors.

Conflict-of-interest disclosure: G.S.V. is a consultant to STRM.BIO and holds a research grant from AstraZeneca (G113590) that funded part of the research presented here. K.T. has received stock options and research funding from Storm Therapeutics Ltd. O.T. is an AstraZeneca employee and shareholder. The remaining authors declare no competing financial interests.

ORCID profiles: A.D., 0009-0001-1925-3441; R.W., 0000-0001-5129-7295; M. Gozdecka, 0000-0002-3134-1276; G.G., 0000-0003-1390-6592; R.A., 0000-0001-5077-3798; M.E., 0000-0002-1842-5838; C.R., 0000-0002-3332-4525; V.M.-D.M., 0000-0003-1878-9129; F.V., 0000-0002-0063-4404; A. Sahal, 0000-0003-4755-2884; B.V., 0000-0003-1956-2778; A. Sawle, 0000-0002-2985-5059; E.Y., 0000-0003-2913-0012; J. Russell, 0000-0002-9431-8428; C.H., 0000-0002-9596-7833; J.-E.S., 0000-0002-6704-2032; K.T., 0000-0002-4865-7648; B.J.P.H., 0000-0003-0312-161X; A.J.W., 0000-0001-9277-4553; G.S.V., 0000-0003-4337-8022.

Correspondence: George S. Vassiliou, Department of Haematology, Cambridge Stem Cell Institute, University of Cambridge, Puddicombe Way, Cambridge, CB2 0AW, United Kingdom; email: gsv20@cam.ac.uk; and Aristi Damaskou, Department of Haematology, Cambridge Stem Cell Institute, University of Cambridge, Puddicombe Way, Cambridge, CB2 0AW, United Kingdom; email: ad971@cam.ac.uk.

Footnotes

Submitted 12 July 2024; accepted 21 May 2025; prepublished online on *Blood* First Edition 25 June 2025. https://doi.org/10.1182/blood.2024026113.

RNA sequencing data have been deposited in the Gene Expression Omnibus database (accession numbers GSE264084 and GSE264322).

Mass spectrometry proteomics data have been deposited in the ProteomeXchange Consortium (data set identifier PXD053249).

Data are available on request from the corresponding authors, George S. Vassiliou (gsv20@cam.ac.uk) and Aristi Damaskou (ad971@cam.ac.uk).

The online version of this article contains a data supplement.

There is a *Blood* Commentary on this article in this issue.

The publication costs of this article were defrayed in part by page charge payment. Therefore, and solely to indicate this fact, this article is hereby marked "advertisement" in accordance with 18 USC section 1734.

REFERENCES

1. Yu Y, Maggi LB Jr, Brady SN, et al. Nucleophosmin is essential for ribosomal protein L5 nuclear export. *Mol Cell Biol*. 2006;26(10):3798-3809.
2. Colombo E, Marine JC, Danovi D, Falini B, Pelicci PG. Nucleophosmin regulates the stability and transcriptional activity of p53. *Nat Cell Biol*. 2002;4(7):529-533.
3. Itahana K, Bhat KP, Jin A, et al. Tumor suppressor ARF degrades B23, a nucleolar protein involved in ribosome biogenesis and cell proliferation. *Mol Cell*. 2003;12(5):1151-1164.
4. Swaminathan V, Kishore AH, Febitha KK, Kundu TK. Human histone chaperone Nucleophosmin enhances acetylation-dependent chromatin transcription. *Mol Cell Biol*. 2005;25(17):7534-7545.
5. Lee SY, Park J-H, Kim S, Park EJ, Yun Y, Kwon J. A proteomics approach for the identification of nucleophosmin and heterogeneous nuclear ribonucleoprotein C1/C2 as chromatin-binding proteins in response to DNA double-strand breaks. *Biochem J*. 2005;388(Pt 1):7-15.
6. Okuda M. The role of nucleophosmin in centrosome duplication. *Oncogene*. 2002;21(40):6170-6174.
7. Dörner K, Ruggeri C, Zemp I, Kutay U. Ribosome biogenesis factors—from names to functions. *EMBO J*. 2023;42(7):e112699.
8. Feric M, Vaidya N, Harmon TS, et al. Coexisting liquid phases underlie nucleolar sub-compartments. *Cell*. 2016;165(7):1686-1697.
9. Mitrea DM, Cika JA, Guy CS, et al. Nucleophosmin integrates within the nucleolus via multi-modal interactions with proteins displaying R-rich linear motifs and rRNA. *Elife*. 2016;5:e13571.
10. Mitrea DM, Cika JA, Stanley CB, et al. Self-interaction of NPM1 modulates multiple mechanisms of liquid-liquid phase separation. *Nat Commun*. 2018;9(1):842.
11. Nachmani D, Bothmer AH, Grisendi S, et al. Germline NPM1 mutations lead to altered rRNA 2′-O-methylation and cause dyskeratosis congenita. *Nat Genet*. 2019;51(10):1518-1529.
12. Falini B, Mecucci C, Tiacci E, et al. Cytoplasmic nucleophosmin in acute myelogenous leukemia with a normal karyotype. *N Engl J Med*. 2005;352(3):254-266.
13. Papaemmanuil E, Gerstung M, Bullinger L, et al. Genomic classification and prognosis in acute myeloid leukemia. *N Engl J Med*. 2016;374(23):2209-2221.
14. Falini B, Bolli N, Liso A, et al. Altered nucleophosmin transport in acute myeloid leukaemia with mutated NPM1: molecular basis and clinical implications. *Leukemia*. 2009;23(10):1731-1743.

15. Döhner K, Thiede C, Jahn N, et al. Impact of NPM1/FLT3-ITD genotypes defined by the 2017 European LeukemiaNet in patients with acute myeloid leukemia. *Blood*. 2020;135(5):371-380.

16. Stone RM, Mandrekar SJ, Sanford BL, et al. Midostaurin plus Chemotherapy for Acute Myeloid Leukemia with a FLT3 Mutation. *N Engl J Med*. 2017;377(5):454-464.

17. Short NJ, Konopleva M, Kadia TM, et al. Advances in the treatment of acute myeloid leukemia: New drugs and new challenges. *Cancer Discov*. 2020;10(4):506-525.

18. Ranieri R, Pianigiani G, Sciabolacci S, et al. Current status and future perspectives in targeted therapy of NPM1-mutated AML. *Leukemia*. 2022;36(10):2351-2367.

19. Yun H, Narayan N, Vohra S, et al. Mutational synergy during leukemia induction remodels chromatin accessibility, modification and 3-Dimensional DNA topology to alter gene expression. *Nat Genet*. 2021;53(10):1443-1455.

20. Vassiliou GS, Cooper JL, Rad R, et al. Mutant nucleophosmin and cooperating pathways drive leukemia initiation and progression in mice. *Nat Genet*. 2011;43(5):470-475.

21. Dovey OM, Cooper JL, Mupo A, et al. Molecular synergy underlies the co-occurrence patterns and phenotype of NPM1-mutant acute myeloid leukemia. *Blood*. 2017;130(17):1911-1922.

22. Kramer MH, Zhang Q, Sprung R, et al. Proteomic and phosphoproteomic landscapes of acute myeloid leukemia. *Blood*. 2022;140(13):1533-1548.

23. Tzelepis K, Koike-Yusa H, De Braekeleer E, et al. A CRISPR dropout screen identifies genetic vulnerabilities and therapeutic targets in acute myeloid leukemia. *Cell Rep*. 2016;17(4):1193-1205.

24. Meyers RM, Bryan JG, McFarland JM, et al. Computational correction of copy-number effect improves specificity of CRISPR-Cas9 essentiality screens in cancer cells. *Nat Genet*. 2017;49(12):1779-1784.

25. Dempster JM, Rossen J, Kazachkova M, et al. Extracting biological insights from the project achilles genome-scale CRISPR screens in cancer cell lines. *bioRxiv*. Preprint posted online 31 July 2019. https://doi.org/10.1101/720243

26. Sasaki T, Toh-E A, Kikuchi Y. Yeast Krr1p physically and functionally interacts with a novel essential Kri1p, and both proteins are required for 40S ribosome biogenesis in the nucleolus. *Mol Cell Biol*. 2000;20(21):7971-7979.

27. Ge W, Wolf A, Feng T, et al. Oxygenase-catalyzed ribosome hydroxylation occurs in prokaryotes and humans. *Nat Chem Biol*. 2012;8(12):960-962.

28. Wu S, Tutuncuoglu B, Yan K, et al. Diverse roles of assembly factors revealed by structures of late nuclear pre-60S ribosomes. *Nature*. 2016;534(7605):133-137.

29. Hua Y, Song J, Peng C, et al. Advances in the relationship between regulator of ribosome synthesis 1 (RRS1) and diseases. *Front Cell Dev Biol*. 2021;9:620925.

30. O'Leary MN, Schreiber KH, Zhang Y, et al. The ribosomal protein Rpl22 controls ribosome composition by directly repressing expression of its own paralog, Rpl22l1. *PLoS Genet*. 2013;9(8):e1003708.

31. Falini B, Gionfriddo I, Cecchetti F, Ballanti S, Pettirossi V, Martelli MP. Acute myeloid leukemia with mutated nucleophosmin (NPM1): any hope for a targeted therapy? *Blood Rev*. 2011;25(6):247-254.

32. Falini B, Brunetti L, Martelli MP. Dactinomycin in NPM1 -mutated acute myeloid leukemia. *N Engl J Med*. 2015;373(12):1180-1182.

33. Gionfriddo I, Brunetti L, Mezzasoma F, et al. Dactinomycin induces complete remission associated with nucleolar stress response in relapsed/refractory NPM1-mutated AML. *Leukemia*. 2021;35(9):2552-2562.

34. Burger K, Mühl B, Harasim T, et al. Chemotherapeutic drugs inhibit ribosome biogenesis at various levels. *J Biol Chem*. 2010;285(16):12416-12425.

35. Lafita-Navarro MC, Conacci-Sorrell M. Nucleolar stress: from development to cancer. *Semin Cell Dev Biol*. 2023;136:64-74.

36. Potapova TA, Unruh JR, Conkright-Fincham J, et al. Distinct states of nucleolar stress induced by anticancer drugs. *Elife*. 2023;12:RP88799.

37. Yung BY, Chang F-J, Bor AM, Lee ES. Schedule-dependent effects of two consecutive, divided, low doses of actinomycin D on translocation of protein B23, inhibition of cell growth and RNA synthesis in hela cells. *Int J Cancer*. 1992;52(2):317-322.

38. Ferreira R, Schneekloth JS, Panov KI, Hannan KM, Hannan RD. Targeting the RNA polymerase I transcription for cancer therapy comes of age. *Cells*. 2020;9(2):266.

39. Peltonen K, Colis L, Liu H, et al. A targeting modality for destruction of RNA polymerase I that possesses anticancer activity. *Cancer Cell*. 2014;25(1):77-90.

40. Drygin D, Lin A, Bliesath J, et al. Targeting RNA polymerase I with an oral small molecule CX-5461 inhibits ribosomal RNA synthesis and solid tumor growth. *Cancer Res*. 2011;71(4):1418-1430.

41. Dinardo CD, Pratz K, Pullarkat V, et al. Venetoclax combined with decitabine or azacitidine in treatment-naive, elderly patients with acute myeloid leukemia. *Blood*. 2019;133(1):7-17.

42. Lachowiez CA, Loghavi S, Kadia TM, et al. Outcomes of older patients with NPM1-mutated AML: Current treatments and the promise of venetoclax-based regimens. *Blood Adv*. 2020;4(7):1311-1320.

43. Weidenauer K, Schmidt C, Rohde C, et al. The ribosomal protein S6 kinase alpha-1 (RPS6KA1) induces resistance to venetoclax/azacitidine in acute myeloid leukemia. *Leukemia*. 2023;37(8):1611-1625.

44. Sapkota GP, Cummings L, Newell FS, et al. BI-D1870 is a specific inhibitor of the p90 RSK (ribosomal S6 kinase) isoforms in vitro and in vivo. *Biochem J*. 2007;401(1):29-38.

45. Babaian A, Rothe K, Girodat D, et al. Loss of m 1 acp 3 J Ribosomal RNA Modification Is a Major Feature of Cancer. *Cell Rep*. 2020;31(5):107611.

46. Meyer B, Wurm JP, Sharma S, et al. Ribosome biogenesis factor Tsr3 is the aminocarboxypropyl transferase responsible for 18S rRNA hypermodification in yeast and humans. *Nucleic Acids Res*. 2016;44(9):4304-4316.

47. Uckelmann HJ, Haarer EL, Takeda R, et al. Mutant NPM1 directly regulates oncogenic transcription in acute myeloid leukemia. *Cancer Discov*. 2023;13(3):746-765.

48. Wang XQD, Fan D, Han Q, et al. Mutant NPM1 hijacks transcriptional hubs to maintain pathogenic gene programs in acute myeloid leukemia. *Cancer Discov*. 2023;13(3):724-745.

49. Kim H, Kim G, Park HJ, Lee MJ, Park Y, Jang S. Integrating holotomography and deep learning for rapid detection of NPM1 mutations in AML. *Sci Rep*. 2024;14(1):23780.

50. Wu H-C, Rérolle D, Berthier C, et al. Actinomycin D targets NPM1c-primed mitochondria to restore PML-driven senescence in AML therapy. *Cancer Discov*. 2021;11(12):3198-3213.

51. Lohrum MAE, Ludwig RL, Kubbutat MHG, Hanlon M, Vousden KH. Regulation of HDM2 activity by the ribosomal protein L11. *Cancer Cell*. 2003;3(6):577-587.

52. Horn HF, Vousden KH. Cooperation between the ribosomal proteins L5 and L11 in the p53 pathway. *Oncogene*. 2008;27(44):5774-5784.

53. Zheng J, Lang Y, Zhang Q, et al. Structure of human MDM2 complexed with RPL11 reveals the molecular basis of p53 activation. *Genes Dev*. 2015;29(14):1524-1534.

54. Nechiporuk T, Kurtz SE, Nikolova O, et al. The TP53 apoptotic network is a primary mediator of resistance to BCL2 inhibition in AML cells. *Cancer Discov*. 2019;9(7):910-925.

55. Pan R, Ruvolo V, Mu H, et al. Synthetic lethality of combined Bcl-2 inhibition and p53 activation in AML: mechanisms and superior antileukemic efficacy. *Cancer Cell*. 2017;32(6):748-760.e6.